

The BiomolBiomed publishes an “Advanced Online” manuscript format as a free service to authors in order to expedite the dissemination of scientific findings to the research community as soon as possible after acceptance following peer review and corresponding modification (where appropriate). An “Advanced Online” manuscript is published online prior to copyediting, formatting for publication and author proofreading, but is nonetheless fully citable through its Digital Object Identifier (doi®). Nevertheless, this “Advanced Online” version is NOT the final version of the manuscript. When the final version of this paper is published within a definitive issue of the journal with copyediting, full pagination, etc., the new final version will be accessible through the same doi and this “Advanced Online” version of the paper will disappear.

## RESEARCH ARTICLE

*Zhang et al: Sputum KL-6 and HRCT in IPF*

# Induced sputum KL-6 combined with HRCT scoring for diagnosing and monitoring idiopathic pulmonary fibrosis

Bingxin Zhang\*, Dejun Zhao, Danping Hu

The second department of respiration, the First People’s Hospital of Fuyang District, Hangzhou, China

\*Correspondence to Bingxin Zhang: [bingxinzhangbxz@163.com](mailto:bingxinzhangbxz@163.com)

DOI: <https://doi.org/10.17305/bb.2025.12667>

## ABSTRACT

Idiopathic pulmonary fibrosis (IPF) is a progressive and fatal interstitial lung disease for which reliable early diagnostic biomarkers are still lacking. This study aimed to evaluate the diagnostic and monitoring value of induced sputum Krebs von den Lungen-6 (KL-6) levels in patients with IPF and to investigate their relationship with pulmonary function parameters and high-resolution computed tomography (HRCT) scoring. In this prospective observational study, 20 patients with IPF and 20 age-matched healthy subjects (HS) were enrolled between October 2021 and April 2023. Induced sputum samples were collected for KL-6 measurement using enzyme-linked immunosorbent assay, while all participants underwent pulmonary function testing and HRCT scoring. KL-6 levels were significantly higher in the IPF group compared with the HS group [776.29 (interquartile range, IQR: 681.98–858.57) vs. 322.21 (IQR: 253.67–338.64) U/mL,  $p<0.001$ ]. In IPF patients, induced sputum KL-6 levels showed strong negative correlations with multiple lung function indices, including forced expiratory volume in one second (FEV1), forced vital capacity (FVC), and diffusing capacity for carbon monoxide (DL<sub>CO</sub>) (all  $p<0.05$ ), and a strong positive correlation with HRCT scores ( $r=0.908$ ,  $p<0.001$ ). Receiver operating characteristic (ROC) analysis demonstrated that combining KL-6 levels with HRCT scores yielded an area under the curve (AUC) of 0.936 (95% confidence interval, CI: 0.914–0.944), with specificity of 97.5% and sensitivity of 80.0%. In conclusion, induced sputum KL-6 levels reflect the degree of pulmonary fibrosis and are closely associated with functional and imaging indicators in IPF. The combination of KL-6 with HRCT scoring enhances diagnostic accuracy, underscoring its potential clinical utility as a noninvasive biomarker for early detection and monitoring of IPF.

**Keywords:** Diagnosis, high-resolution computed tomography score, idiopathic pulmonary fibrosis, induced sputum, Krebs von den Lungen-6.

## INTRODUCTION

Idiopathic Pulmonary Fibrosis (IPF) is a progressive and irreversible form of interstitial lung disease (ILD), characterized by alveolar structure damage, abnormal deposition of fibrous tissue, and persistent inflammatory responses(1). As the disease progresses, lung tissue architecture is disrupted, leading to impaired gas exchange and a gradual decline in pulmonary function, which may ultimately result in respiratory failure or even death(2). Clinically, patients often present with progressive dyspnea, dry cough, worsening pulmonary function, and reticular or honeycomb-like imaging abnormalities predominantly in the lower lung zones(3, 4). High-resolution computed tomography (HRCT) plays a crucial role in IPF diagnosis, typically revealing basal-predominant honeycombing and interstitial abnormalities(5-7). IPF affects approximately 3 million people worldwide, with incidence rates increasing significantly with age(8). Currently, aside from lung transplantation, treatment strategies primarily focus on slowing disease progression and preventing respiratory failure(9). The median survival after diagnosis is only 3-5 years(10), and the natural course of the disease is highly variable and unpredictable. Thus, early diagnosis and intervention are critical for improving patient outcomes. However, the lack of reliable early diagnostic biomarkers remains a major obstacle in the precise management and treatment of IPF. Identifying novel, more sensitive, and specific biomarkers is essential for improving early detection rates.

Krebs von den Lungen-6 (KL-6), a glycoprotein encoded by the *MUC1* gene, is predominantly expressed on type II alveolar epithelial cells(11, 12). Studies have shown that serum and bronchoalveolar lavage fluid (BALF) KL-6 levels are significantly elevated in IPF patients and negatively correlate with pulmonary function parameters such as FVC and DLCO%(13, 14). Moreover, sputum KL-6 levels strongly correlate with the degree of pulmonary function impairment, indicating its potential clinical utility(15). However, serum and natural sputum still have certain limitations in reflecting lesions of the lung, especially of the lower respiratory tract. Induced sputum, as airway secretions obtained through saline

nebulization stimulation, can more effectively represent the local pathological state of the lower respiratory tract and provide more direct and sensitive biological information. Therefore, investigating the role of induced sputum KL-6 in IPF diagnosis and disease monitoring may provide a more accurate biomarker for clinical use. Based on this evidence, the present study aims to evaluate the potential clinical utility of induced sputum KL-6 as a potential biomarker for IPF diagnosis by examining its associations with pulmonary function indices and HRCT imaging scores in IPF patients.

## **MATERIALS AND METHODS**

### **Study population**

This study was designed as a prospective observational study. Between October 2021 and April 2023, we consecutively recruited eligible participants from our institution, enrolling a total of 40 subjects comprising 20 IPF patients (IPF group) and 20 healthy subjects (HS group). The inclusion criteria of the IPF group were as follows: patients aged  $\geq 20$  years; the diagnostic criteria for IPF were set by utilizing the 2018 American Thoracic Society/European Respiratory Society (ATS/ERS) criteria(7) and diagnostic and treatment guidelines developed by the Respiratory Diseases Section of the Chinese Medical Association(16); the main manifestations of CT were ground-glass-like lesions, honeycomb pattern, streaks, lattice shadows, and solid shadows; patients who were first diagnosed with IPF and had no systemic anti-fibrotic treatment; patients who were informed about the study treatment, mentally well and with normal consciousness. The exclusion criteria were as follows: patients with IPF combined with chronic obstructive pulmonary disease (COPD), IPF combined with emphysema, IPF combined with pulmonary infection, and IPF combined with acute lung injury; patients with secondary ILDs such as Connective Tissue Disease-associated ILD (CTD-ILD), occupational or environmental exposures, chronic hypersensitivity pneumonitis, etc; and patients who were pregnant and lactating women. The healthy subjects were recruited from the health examination

population of our hospital's physical examination center during the same period as IPF patients, with the inclusion criteria being age-matched IPF groups, no lung disease or other major systemic diseases, no respiratory symptoms in the latest one week, and no history of drug use. The program is shown in Figure 1. The work received approval from the Ethics Committee of our hospital (2020016). Before the participation, each patient signed an informed consent form.

In the process of disease diagnosis, we organized multidisciplinary discussions, with the participation of the director of rheumatology and immunology, the attending physician of the imaging department, and respiratory specialists. By comprehensively analyzing the patient's clinical symptoms, physical examination, rheumatoid immune antibody results, and HRCT imaging findings, for patients with usual interstitial pneumonia (UIP) or possible images of UIP patterns, the clinical diagnosis of IPF was ultimately reached after excluding rheumatic immune diseases.

Sample size estimation was performed using G\*Power software based on an independent samples *t*-test model. With the following parameters: effect size (Cohen's *d*) of 0.9,  $\alpha$  level of 0.05, and power of 0.80, the calculation indicated that a minimum of 20 participants per group (total sample size of 40) would be required.

## **Research program**

### *Sample collection and KL-6 testing*

Patients inhaled salbutamol 400  $\mu$ g before the collection of induced sputum to expand the bronchus. They then inhaled hypertonic solution (5% NaCl) for the induction of sputum. The forced expiratory volume per second (FEV1) was monitored throughout the induction. If there was a decrease of more than 20% in FEV1 from baseline, the operation was stopped to ensure the safety of patients. After gathering the entire sputum in a plastic container, it was weighed and vortexed for 30 s by adding three times the volume of phosphate-buffered saline (PBS) solution. It was then centrifuged at 800 g for 10 min at 4 °C. After supernatant separation, the samples were kept at -80 °C(17, 18). During the sputum processing, dithiothreitol was not used, but the viscosity was effectively reduced by diluting with PBS and vortex mixing,

ensuring the suitability of the sample. Samples with less than 20% squamous cells were considered eligible for the study(19).

With the use of the KL-6 enzyme immunoassay kit (Bioswamp, China), we assessed the levels of KL-6 in sputum samples. Firstly, we used the serial dilution test to construct the concentration gradient of the standard substance. The original concentration standard substance was sequentially diluted into six groups of concentrations of 1800, 900, 450, 225, 112.5, and 0 U/mL. Two parallel wells were set for each concentration in the ELISA plate, and a calibration curve was established based on the results. Subsequently, we added 40  $\mu$ L of the sample and 10  $\mu$ L of biotinylated anti-KL-6 antibody to the test sample well, and performed the same procedure in the blank control well, except for the addition of the sample and antibody. 50  $\mu$ L of ELISA reagent was added to the reaction wells. The wells were incubated in a 37 °C water bath for 30 min. The solution was discarded, and the plate was washed 5 times with a 30-fold diluted washing solution. Then we added 50  $\mu$ L of developer A and developer B to each well in sequence, mixed them well, and incubated them in the dark at 37 °C for 10 min. We added 50  $\mu$ L of termination solution to stop the reaction, and the color changed into yellow from blue. Finally, the OD of the blank wells was set as 0. We measured the OD values of each well at a wavelength of 450 nm within 15 min and calculated the concentration of KL-6 in the sample based on the standard curve. The precision was evaluated using low-level quality control (CV=3.95%) and high-level quality control (CV=3.12%), with an overall intra-batch  $CV \leq 8.0\%$  and inter-batch  $CV \leq 15.0\%$ , indicating good repeatability and reproducibility of the method.

#### *Tests for pulmonary function*

We launched pulmonary function tests in compliance with the guidelines of the American Thoracic Society(20). By utilizing the Viasys Master Screen Vegeta/DFP (Viasys Healthcare GmbH, Höchberg, Germany), we conducted standard spirometry for all patients and measured parameters including forced vital capacity (FVC), FEV1, and the ratio of Forced Expiratory Volume in one second to FVC (FEV1/FVC),

Diffusing capacity of the lung for carbon monoxide (DL<sub>CO</sub>), to evaluate lung diffusion function, with all expressed as a percentage of actual and predicted values. FEV1%pred values over 70% were considered as normal, 60-70% as mild impairment, 50-60% as moderate impairment, and below 50% as severe impairment. DL<sub>CO</sub>%pred values over 80% were considered as normal, 60-80% as mild impairment, 40-60% as moderate impairment, and below 40% as severe impairment.

### *HRCT score*

All patients underwent lung HRCT scanning using a 64-row, 128-slice CT computed tomography system (MDCT, Siemens Somatom Definition 128-slice CT system; Siemens, Germany). CT images and imaging parameters were consistent for all patients: tube voltage of 120 kVp, scan collimation of 128×0.6 or 256×0.6 mm, tube current modulation, reconstructed slice thickness of 1.5 mm, and the gantry rotation speed of 0.5 s/r. The scan range extended from the lung apices to the lower half of the diaphragm.

HRCT images of the IPF group of patients were scored by two radiologists with 2 or more years of work experience. The mean value was regarded as the final result. Fibrosis score was determined at six levels. The lungs of patients were divided into six regions, including the above part of the aortic arch, the part below the aortic arch to the right pulmonary vein, and the part below the right pulmonary vein (upper, middle, and lower lung zones)(21). By employing the international HRCT grading method(22, 23), the interstitial abnormalities score for each lung zone ranged from 0 to 5, with a total score of 30. The specific scoring criteria were as follows: score 0 (no obvious interstitial changes were detected); score 1 (abnormalities of lobular structure such as subpleural arc shadow, subpleural vertical line shadow, etc); score 2 (abnormalities of interstitial shadow around the bronchial vascular bundles, thickening of bronchial vascular bundles, deformation of lobular contour, and lobular septum); score 3 (abnormalities of lobular morphology accompanied by abnormalities of interstitial shadow around the bronchial vascular bundles with a <10 mm honeycomb shadow); score 4 (the range of honeycomb shadow was expanded to

10-30 mm based on the above statues); score 5 (abnormal interstitial shadow around the small bronchial vascular bundles, the range of honeycomb shadow >30mm, with unclear or disappeared lung texture). Patients' HRCT scores were cumulative of the fibrosis scores for each lung region. The degree of pulmonary fibrosis in patients was quantitatively analyzed and calculated based on HRCT images.

### **Ethics approval and consent to participate**

The study was approved by the ethics committee of the First People's Hospital of Fuyang District (2020016). The methods were carried out in accordance with the approved guidelines.

### **Statistical analysis**

Data were processed by IBM SPSS 26.0 (IBM Corporation, USA) statistical software. All measurement data were first evaluated for normality using the Shapiro-Wilk test. Quantitative data that conformed to a normal distribution were expressed as mean  $\pm$  standard deviation (SD). The independent sample *t*-test was used for comparison between two groups. Quantitative data that did not conform to normal distribution were represented by median (quartiles) [M (P25, P75)]. Non-parametric Mann-Whitney U test was used for comparison between two groups, and ANOVA was used for multi-group comparison. The count data was represented as N (%), and the comparison between groups was conducted using  $\chi^2$  test. All tests were bilateral tests, with  $P < 0.05$  indicating statistical differences. Given that HRCT score was an ordered graded variable, Spearman correlation analysis was used to determine the correlation between induced sputum KL-6 levels and lung function, as well as the HRCT score. Receiver operating characteristic (ROC) curve analysis was used to evaluate the efficacy of induced sputum KL-6 and combined HRCT score in diagnosing idiopathic pulmonary fibrosis. The diagnostic accuracy was quantified by calculating the Area Under the Curve (AUC), and the ROC threshold was determined by the maximum Youden index. To reduce the risk of model overfitting and result bias, this study conducted internal validation of the ROC curve using the bootstrap method with 1000 repeated samples to obtain robust estimates of AUC and its 95%



confidence interval (CI), thereby improving the reliability of diagnostic efficacy evaluation.

## RESULTS

### Baseline characteristics of patients

The clinical characteristics of patients in the two groups were analyzed (Table 1). In the IPF group with a median age of 73.00 years, 15 (75.0%) were male, 5 (25.0%) were female, and the BMI was  $24.77 \pm 5.15$  kg/m<sup>2</sup>. 12 patients had a history of smoking. 14 patients had comorbidities (some patients had multiple diseases), including 6 cases of hypertension, 9 cases of diabetes, and 6 cases of coronary heart disease. The median SpO<sub>2</sub> of IPF group patients was significantly lower than that of the healthy group (92.00 vs. 97.00,  $P < 0.001$ ), and there was a significant difference in HRCT scores between the two groups (9.00 vs. 0.5,  $P < 0.001$ ). No significant differences in age, gender, BMI, smoking history, comorbidities, and C-reactive protein (CRP) among the two groups were detected ( $P > 0.05$ ).

### Induced sputum KL-6 is greatly elevated in IPF patients

The IPF group demonstrated significantly higher KL-6 levels in induced sputum 776.29 (IQR: 681.98, 858.57) U/mL compared to the HS group [322.21 (IQR: 253.67, 338.64) U/mL,  $P < 0.001$ ] (Figure 2A). When stratifying IPF patients by GAP index severity stages, KL-6 levels showed differences across stages: Stage I 690.44 (IQR: 518.20, 790.65) U/mL, Stage II 804.39 (IQR: 734.42, 820.83) U/mL, and Stage III 1104.60 (IQR: 1104.60, NA) U/mL, with statistically significant differences among groups (Figure 2B,  $P < 0.05$ ).

### Relationship between induced sputum KL-6 and lung function and HRCT score in the IPF group

In the IPF group, the levels of induced sputum KL-6 were significantly negatively linked to lung function parameters FEV1 ( $r = -0.470$ ,  $P = 0.037$ ), FVC ( $r = -0.496$ ,  $P = 0.026$ ), FEV1%pred ( $r = -0.711$ ,  $P < 0.001$ ), FVC%pred ( $r = -0.625$ ,

$P=0.003$ ),  $DL_{CO}\%$  ( $r=-0.686$ ,  $P<0.001$ ),  $DL_{CO}\%pred$  ( $r=-0.783$ ,  $P<0.001$ ) and  $DL_{CO}/VA\%$  ( $r=-0.872$ ,  $P<0.001$ ), indicating a close linkage between elevated induced sputum KL-6 levels and decreased lung function. However, there was a significant positive correlation between induced sputum KL-6 and HRCT score ( $r=0.908$ ,  $P<0.001$ ) (Figure 3, Supplementary Table 1).

### **Analysis of induced sputum KL-6 and the extent of lung fibrosis on HRCT in the IPF group**

The lung fibrosis status of Patient 1 was analyzed (Figure 4A-B), with HRCT showing a lung fibrosis extent of 15.9% and a KL-6 level of 820.83 U/mL. The HRCT images of the lungs of Patient 2 showed a total lung fibrosis extent of 31.3% and a KL-6 level of 1002.63 U/mL (Figure 4C-D).

### **ROC curves of induced sputum KL-6 combined with HRCT score**

The ROC curves demonstrated that when the KL-6 level in the induced sputum reached 623.78 U/mL, the sensitivity for distinguishing whether IPF occurred in the patient was 90.0%, the specificity was 67.5%, and the AUC was 0.844 (Figure 5). With an HRCT score of 7.75, patients had a specificity of 85.0%, a sensitivity of 80.0%, and an AUC of 0.899 for the development of IPF. In contrast, the model 1 had a specificity of 97.5% and a sensitivity of 80.0%, with an AUC of 0.936 (95%CI: 0.914, 0.944) when the two were combined for diagnosis. In addition, we also adjusted for confounding factors (age and smoking status) in the joint diagnosis. The sensitivity of Model 2 was 80.0%, specificity was 97.5%, and AUC was 0.940 (95% CI: 0.874, 0.956) (Table 2).

## **DISCUSSION**

The project aimed to evaluate the potential function of KL-6 in induced sputum in IPF diagnosis and assessment, and to investigate its relationship with pulmonary function parameters and HRCT scores. Comparative analysis between the IPF and HS groups revealed significantly elevated levels of KL-6 in induced sputum from IPF

patients ( $P < 0.001$ ), with increasing concentrations observed alongside disease severity progression. Furthermore, induced sputum KL-6 demonstrated a significant negative correlation with pulmonary function parameters (FEV1, FVC, FEV1%pred, FVC%pred, DL<sub>CO</sub>%, DL<sub>CO</sub>%pred, and DL<sub>CO</sub>/VA%) ( $P < 0.05$ ) and a significant positive correlation with HRCT scores ( $P < 0.001$ ). Additionally, the diagnostic efficacy of KL-6 combined with HRCT scores was significantly higher, with an AUC as high as 0.936 (95%CI: 0.914, 0.944) with a sensitivity and specificity of 80.0% and 97.5%, respectively.

Patients with IPF exhibited elevated KL-6 levels due to extensive damage and fibrosis of alveolar epithelial cells, which provided a key basis for early diagnosis and disease monitoring of IPF. The level of KL-6 in induced sputum was higher than the IPF group in this study, which is consistent with the results of former studies on KL-6 as a marker of ILD(11, 24, 25). Elevated KL-6 levels can reflect the severity and ILD progression(26). As revealed by a meta-analysis, the KL-6 level in severe ILD patients is 703.41 U/mL, which is higher than that in mild patients, while the KL-6 level in progressive ILD patients is 325.98 U/mL, which is more elevated than that in non-progressive patients(27). In addition, KL-6 levels also affect prognosis. Yokoyama *et al.*(26) revealed that patients with IPF who have low KL-6 levels often live for over 36 months, but those who have high KL-6 levels typically live for only 18 months, suggesting that the assessment of serum KL-6 levels can predict the survival rate of IPF patients. We hypothesized the possible reasons for KL-6 elevation. First, the pathologic damage forms of IPF-ILD are diverse, of which the most common types are pulmonary vascular epithelial damage and diffuse alveolar epithelial cell damage. These injuries can induce chronic fibrosis(28). Secondly, KL-6 is an immunoglobulin glycoprotein mainly modulated by the *MUC1* gene, exhibiting high expression on proliferating Alveolar Epithelial Cell II (AECII). When AEC II is damaged or regenerated, KL-6 on the cell membrane is easily sheared and released into the alveolar cavity and airway secretions; If the alveolar capillary barrier is damaged, it can enter the bloodstream(29, 30). Thirdly, in severe IPF-ILD, extensive inflammatory response and inflammatory exudate of degenerative AECII not only

lead to an expansion of lung parenchyma visible on HRCT, but also stimulate the release of KL-6 from more AECII(31).

Induced sputum KL-6 levels were considerably inversely linked with lung function parameters (FEV1, FVC, FEV1%pred, FVC%pred, DL<sub>CO</sub>%, DLCO%pred and DL<sub>CO</sub>/VA%), indicating that KL-6 can not only reflect the degree of lung inflammation and damage but also impact the actual lung function of patients, suggesting that KL-6 levels can function as a pivotal indicator for evaluating the extent of lung function impairment in IPF patients. Sokai *et al.*(32) pointed out that changes in serum KL-6 levels over 6 months were significantly linked to changes in FVC ( $r=-0.38$ ,  $p<0.01$ ) and DLCO% ( $r=-0.33$ ,  $p=0.01$ ) in patients with IPF. Furthermore, a case-control study manifested that elevated serum KL-6 levels exhibited negative links with FVC ( $r=-0.93$ ) and FEV1 ( $r=-0.91$ )(33). These results all supported the potential of KL-6 as an instrumental biomarker for lung function assessment.

Moreover, induced sputum levels of KL-6 were greatly positively linked with HRCT scores ( $P<0.001$ ). This finding is in line with the results of Wang *et al.*(34), which suggested that KL-6 levels reflect the degree of fibrosis on imaging and that the detection of KL-6 by induced sputum simplifies the complexity of disease monitoring. Our study presented two patients with typical UIP images. HRCT image of patient 1 showed a degree of pulmonary fibrosis of 15.9% and KL-6 levels of 820.83 U/mL. The degree of pulmonary fibrosis in patient 2 was 31.3%, and the KL-6 level increased to 1002.63 U/mL, indicating that the KL-6 level showed a consistent upward trend with the fibrosis range evaluated by HRCT. We speculated that the possible reason is that the elevation of KL-6, as a high molecular weight glycoprotein secreted by alveolar type II cells, can reflect the damage and regeneration of alveolar epithelial cells. Patients with higher levels of fibrosis (such as patient 2) often experienced more extensive alveolar epithelial damage and remodeling, resulting in increased secretion of KL-6 and significantly elevated detection levels. These two cases suggested that induced sputum KL-6 detection can not only reflect local

pathological changes in the lower respiratory tract, but may also be closely related to the fibrosis range evaluated by imaging.

The superior diagnostic ability of KL-6 in ILD was also validated, with ROC curves demonstrating 76.36% sensitivity and 91.07% specificity(34). This indicated that induced sputum KL-6 possessed higher sensitivity, further supporting its potential as a reliable marker reflecting the degree of lung fibrosis. Furthermore, Ohshimo *et al.*(24) demonstrated that serum KL-6 levels >1300 U/mL could serve as a predictive biomarker for acute exacerbation of IPF, with a sensitivity of 92% and specificity of 61%. In our ROC analysis, the level of induced sputum KL-6 reached 623.78 U/mL, the sensitivity for distinguishing IPF patients was 90.0%, the specificity was 67.5%, and the AUC was 0.844. When combined with HRCT scoring analysis, the specificity further increased, with AUC reaching 0.943, significantly improving the accuracy of diagnosis. Although the combined application of KL-6 and HRCT scoring significantly improved AUC, its clinical value is not only reflected in the improvement of statistical indicators, but also in the complementary advantages of the two in biological markers and imaging manifestations. In addition, we further adjusted for factors such as age and smoking status, which still support the result. This suggested that the combined use of induced sputum KL-6 and HRCT scoring has potential for more effective identification of IPF patients, improves the sensitivity and specificity of diagnosis, and provides more comprehensive information support for clinical decision-making.

However, this study also has some limitations. Firstly, the sample size of this study is relatively small. Although we have adopted non-parametric analysis methods and strict inclusion and exclusion criteria to reduce data bias, the results may still be influenced by individual differences. Future research will introduce multivariate regression models through multi-center, large-scale cohorts to further control confounding factors and validate the clinical predictive value discovered in this study. At the same time, external independent cohort validation will be conducted to evaluate the broad applicability of the model. Secondly, the control group in this study consisted only healthy population. Other ILDs or chronic respiratory diseases were

not included as controls, so it is not possible to comprehensively evaluate the differential diagnostic ability of KL-6 in complex clinical scenarios. In the future, we plan to further introduce disease control groups to systematically evaluate the sensitivity and specificity of induced sputum KL-6 in different diseases, and further clarify its practical application value in auxiliary diagnosis. Thirdly, this study did not collect serum KL-6 data synchronously, so it is not yet possible to directly compare the relative advantages of serum and induced sputum KL-6 in diagnosis and disease assessment. In the future, we will conduct comparative studies between serum and induced sputum KL-6 to further clarify their complementarity and practical clinical value. Fourthly, although all patients underwent chest CT examination at the time of enrollment to rule out pulmonary infection, and CRP data were provided to further support the absence of active infection during sampling, procalcitonin data were missing by more than 30% and not analyzed. Therefore, this study still cannot completely rule out the potential impact of inflammation or infection on KL-6 levels. Caution should be taken when interpreting the results. In the future, we plan to combine KL-6 testing with clinical data (including CRP, PCT, symptoms, and imaging results) to clarify the impact of inflammatory confounding factors. Finally, since this study did not incorporate a follow-up, longitudinal dynamic change data of KL-6 could not be systematically collected, which limited the in-depth analysis of its disease progression monitoring and prognostic evaluation value. Future prospective long-term follow-up studies will help to comprehensively evaluate the diagnostic and monitoring potential of KL-6.

## CONCLUSION

This work delves into the potential application of induced sputum KL-6 in the diagnosis and evaluation of IPF, demonstrating that the levels of induced sputum KL-6 are considerably higher in IPF patients than in HS patients. Sputum KL-6 level is closely related to lung function parameters and HRCT scores. The combined application of KL-6 and HRCT score can refine the diagnostic accuracy of IPF,

providing a reference for clinical diagnosis and organization. This project indicates that induced sputum KL-6 can be a potential biomarker for IPF. However, we still need to further validate it in larger sample sizes and multi-center cohorts, and explore its application value in clinical practice to further optimize the diagnosis and management of IPF.

**Conflicts of interest:** Authors declare no conflicts of interest.

**Funding:** The study was supported by Zhejiang Provincial Health Science and Technology Fund (2021RC027).

**Data availability:** All data generated or analyzed during this study are included in this article.

**Submitted:** May 13, 2025

**Accepted:** August 28, 2025

**Published online:** September 12, 2025

## REFERENCE

1. King TE, Jr., Pardo A, Selman M. Idiopathic pulmonary fibrosis. *Lancet*. 2011;378(9807):1949-61.
2. Hewlett JC, Kropski JA, Blackwell TS. Idiopathic pulmonary fibrosis: Epithelial-mesenchymal interactions and emerging therapeutic targets. *Matrix Biol*. 2018;71-72:112-27.
3. Amaral AF, Colares PFB, Kairalla RA. Idiopathic pulmonary fibrosis: current diagnosis and treatment. *J Bras Pneumol*. 2023;49(4):e20230085.
4. Gross TJ, Hunninghake GW. Idiopathic Pulmonary Fibrosis. *New England Journal of Medicine*. 2001;345(7):517-25.
5. Benegas Urteaga M, Ramirez Ruz J, Sanchez Gonzalez M. Idiopathic pulmonary fibrosis. *Radiologia (Engl Ed)*. 2022;64 Suppl 3:227-39.
6. Mengmeng M, Bingpeng G, Qian H. Interpretation of " Idiopathic Pulmonary Fibrosis (an Update) and Progressive Pulmonary Fibrosis in Adults: An Official ATS/ERS/JRS/ALAT Clinical Practice Guideline (2022 Edition)" : Identification and treatment of progressive pulmonary fibrosis. *International Journal of Respiration*. 2023.
7. Raghu G, Remy-Jardin M, Myers JL, Richeldi L, Ryerson CJ, Lederer DJ, et al. Diagnosis of Idiopathic Pulmonary Fibrosis. An Official ATS/ERS/JRS/ALAT Clinical Practice Guideline. *Am J Respir Crit Care Med*. 2018;198(5):e44-e68.
8. Raghu G, Collard HR, Egan JJ, Martinez FJ, Behr J, Brown KK, et al. An official ATS/ERS/JRS/ALAT statement: idiopathic pulmonary fibrosis: evidence-based guidelines for diagnosis and management. *Am J Respir Crit Care Med*. 2011;183(6):788-824.
9. Koudstaal T, Wijsenbeek MS. Idiopathic pulmonary fibrosis. *Presse Med*. 2023;52(3):104166.
10. Lederer DJ, Martinez FJ. Idiopathic Pulmonary Fibrosis. *New England Journal of Medicine*. 2018;378(19):1811-23.



11. Ishikawa N, Hattori N, Yokoyama A, Kohno N. Utility of KL-6/MUC1 in the clinical management of interstitial lung diseases. *Respir Investig*. 2012;50(1):3-13.
12. Kohno N, Awaya Y, Oyama T, Yamakido M, Akiyama M, Inoue Y, et al. KL-6, a mucin-like glycoprotein, in bronchoalveolar lavage fluid from patients with interstitial lung disease. *Am Rev Respir Dis*. 1993;148(3):637-42.
13. Naccache J-M, Gibiot Q, Monnet I, Antoine M, Wislez M, Chouaid C, et al. Lung cancer and interstitial lung disease: a literature review. *Journal of Thoracic Disease*. 2018;10(6):3829-44.
14. Zhu C, Zhao Y, Kong L, Li Z, Kang J. The expression and clinical role of KL-6 in serum and BALF of patients with different diffuse interstitial lung diseases. *CHINESE JOURNAL OF TUBERCULOSIS AND RESPIRATORY DISEASES*. 2016;039(002):93-7.
15. Guiot J, Henket M, Corhay JL, Moermans C, Louis R. Sputum biomarkers in IPF: Evidence for raised gene expression and protein level of IGFBP-2, IL-8 and MMP-7. *PLoS One*. 2017;12(2):e0171344.
16. CTS-ILD. Chinese expert consensus on the diagnosis and treatment of idiopathic pulmonary fibrosis. *Chinese Journal of Tuberculosis and Respiratory Diseases*. 2016;39(6):427-32.
17. Baha A, Yildirim F, Stark M, Kalkanci A, Fireman E, Kokturk N. Is Induced Sputum A Useful Noninvasive Tool in the Diagnosis of Pulmonary Sarcoidosis? *Turk Thorac J*. 2019;20(4):248-52.
18. Foresi A, Leone C, Pelucchi A, Mastropasqua B, Chetta A, D'Ippolito R, et al. Eosinophils, mast cells, and basophils in induced sputum from patients with seasonal allergic rhinitis and perennial asthma: relationship to methacholine responsiveness. *J Allergy Clin Immunol*. 1997;100(1):58-64.
19. Pizzichini MM, Popov TA, Efthimiadis A, Hussack P, Evans S, Pizzichini E, et al. Spontaneous and induced sputum to measure indices of airway inflammation in asthma. *Am J Respir Crit Care Med*. 1996;154(4 Pt 1):866-9.
20. Miller MR, Crapo R, Hankinson J, Brusasco V, Burgos F, Casaburi R, et al. General considerations for lung function testing. *Eur Respir J*. 2005;26(1):153-61.

21. Huuskonen O, Kivisaari L, Zitting A, Taskinen K, Tossavainen A, Vehmas T. High-resolution computed tomography classification of lung fibrosis for patients with asbestos-related disease. *Scand J Work Environ Health*. 2001;27(2):106-12.
22. Wu WJ, Huang WM, Liang CH, Yun CH. Pulmonary vascular volume is associated with DLCO and fibrotic score in idiopathic pulmonary fibrosis: an observational study. *BMC Med Imaging*. 2022;22(1):76.
23. Fraser E, St Noble V, Hoyles RK, Benamore R, Ho LP. Readily accessible CT scoring method to quantify fibrosis in IPF. *BMJ Open Respir Res*. 2020;7(1).
24. Ohshimo S, Ishikawa N, Horimasu Y, Hattori N, Hirohashi N, Tanigawa K, et al. Baseline KL-6 predicts increased risk for acute exacerbation of idiopathic pulmonary fibrosis. *Respir Med*. 2014;108(7):1031-9.
25. Lederer C, Mayer K, Somogyi V, Kriegsmann K, Kriegsmann M, Buschulte K, et al. Krebs von den Lungen-6 as a Potential Predictive Biomarker in Fibrosing Interstitial Lung Diseases. *Respiration*. 2023;102(8):591-600.
26. Yokoyama A, Kondo K, Nakajima M, Matsushima T, Takahashi T, Nishimura M, et al. Prognostic value of circulating KL-6 in idiopathic pulmonary fibrosis. *Respirology*. 2006;11(2):164-8.
27. Zhang T, Shen P, Duan C, Gao L. KL-6 as an Immunological Biomarker Predicts the Severity, Progression, Acute Exacerbation, and Poor Outcomes of Interstitial Lung Disease: A Systematic Review and Meta-Analysis. *Front Immunol*. 2021;12:745233.
28. Kinoshita F, Hamano H, Harada H, Kinoshita T, Igishi T, Hagino H, et al. Role of KL-6 in evaluating the disease severity of rheumatoid lung disease: comparison with HRCT. *Respir Med*. 2004;98(11):1131-7.
29. Hant FN, Ludwicka-Bradley A, Wang HJ, Li N, Elashoff R, Tashkin DP, et al. Surfactant protein D and KL-6 as serum biomarkers of interstitial lung disease in patients with scleroderma. *J Rheumatol*. 2009;36(4):773-80.
30. Atamas SP. FCP (<http://fibro.biobitfield.com/fcp.php>): a bioinformatic tool assisting in PubMed searches for literature on fibrosis-related cytokines. *Arthritis Rheum*. 2003;48(7):2083-4.

31. Elhai M, Hoffmann-Vold AM, Avouac J, Pezet S, Cauvet A, Leblond A, et al. Performance of Candidate Serum Biomarkers for Systemic Sclerosis-Associated Interstitial Lung Disease. *Arthritis Rheumatol.* 2019;71(6):972-82.
32. Sokai A, Tanizawa K, Handa T, Kanatani K, Kubo T, Ikezoe K, et al. Importance of serial changes in biomarkers in idiopathic pulmonary fibrosis. *ERJ Open Res.* 2017;3(3).
33. Fotoh DS, Helal A, Rizk MS, Esaily HA. Serum Krebs von den Lungen-6 and lung ultrasound B lines as potential diagnostic and prognostic factors for rheumatoid arthritis-associated interstitial lung disease. *Clin Rheumatol.* 2021;40(7):2689-97.
34. Wang T, Yao Y, Wang Y, Wei W, Yin B, Huang M, et al. Evaluating the diagnostic and therapeutic significance of KL-6 in patients with interstitial lung diseases. *Heliyon.* 2024;10(7):e27561.

## TABLES AND FIGURES WITH LEGENDS

**Table 1. Baseline clinical characteristics of patients with idiopathic pulmonary fibrosis (IPF) and healthy subjects (HS).**

	IPF ( <i>n</i> =20)	HS ( <i>n</i> =20)	<i>p</i> value
<b>Age (years)</b>	73.00 (67.25, 77.00)	68.50 (63.50, 73.75)	0.184
<b>Sex</b>			0.311
Male	15 (75.0%)	12 (60.0%)	
Female	5 (25.0%)	8 (40.0%)	
<b>BMI (kg/m<sup>2</sup>)</b>	24.77±5.15	23.71±5.43	0.530
<b>Smoke</b>			0.525
Yes	12 (60.0%)	10 (50.0%)	
No	8 (40.0%)	10 (50.0%)	
<b>Complication</b>			1.000
Hypertension	6 (30.00)	7 (35.00)	
Diabetes	9 (45.00)	8 (40.00)	
Coronary heart disease	6 (30.00)	5 (25.00)	
<b>CRP</b>	3.63 (0.46, 9.04)	4.65 (1.66, 8.95)	0.565
<b>SpO<sub>2</sub></b>	92.00 (90.25, 93.75)	97.00 (95.25, 98.75)	<0.001
<b>Pulmonary function parameters</b>			
FEV1	1.45 (1.31, 1.67)	/	
FVC	1.79 (1.59, 2.03)	/	
FEV1/FVC	0.82 (0.79, 0.84)	/	
FEV1 %pred	59.12 (55.72, 63.41)	/	
FVC %pred	68.58 (65.28, 70.48)	/	

DL <sub>CO</sub>	4.21 (3.63, 4.64)	/	
DL <sub>CO</sub> %pred	63.50 (55.00, 71.00)	/	
DL <sub>CO</sub> /VA%	61.50 (56.00, 68.75)	/	
<b>GAP Stage</b>			
I	7 (35.00)	/	
II	11 (55.00)	/	
III	2 (10.00)	/	
<b>HRCT score</b>	9.00 (8.00, 11.00)	0.50 (0.50, 1.38)	<0.001

Abbreviations: IPF: Idiopathic pulmonary fibrosis; HS: Healthy subjects; BMI: Body mass index; CRP: C-reactive protein; SpO<sub>2</sub>: Peripheral capillary oxygen saturation; FEV<sub>1</sub>: Forced expiratory volume in one second; FVC: Forced vital capacity; FEV<sub>1</sub>/FVC: Ratio of forced expiratory volume in one second to forced vital capacity; DL<sub>CO</sub>: Diffusing capacity of the lung for carbon monoxide; DL<sub>CO</sub>/VA%: Diffusing capacity of the lung for carbon monoxide per unit of alveolar volume; GAP: Gender–age–physiology; HRCT: High-resolution computed tomography.

**Table 2. Diagnostic performance of induced sputum KL-6, HRCT score, and combined models for identifying IPF.**

	<b>AUC (95% CI)</b>	<b>Sensitivity</b>	<b>Specificity</b>
<b>KL-6</b>	0.844 (95%CI: 0.741-0.946)	0.900	0.675
<b>HRCT</b>	0.899 (95%CI: 0.818-0.980)	0.800	0.850
<b>Model 1</b>	0.936 (95%CI: 0.914, 0.944)	0.800	0.975
<b>Model 2</b>	0.940 (95%CI: 0.874, 0.956)	0.800	0.975

Note: Model 1: KL-6+HRCT, no adjusted. Model 2: Model 1 + adjusted age and smoke. Abbreviations: AUC: Area under the curve; CI: Confidence interval; KL-6: Krebs von den Lungen-6; HRCT: High-resolution computed tomography.

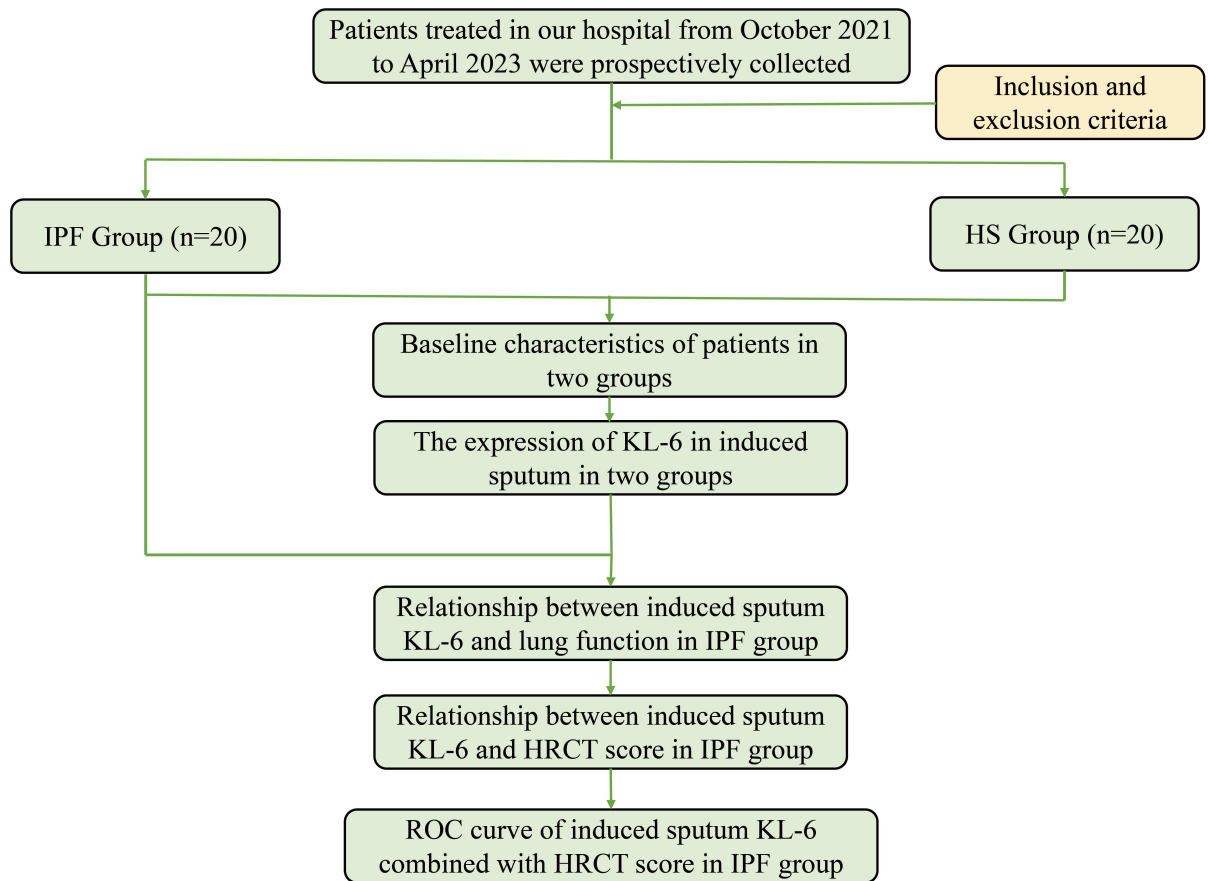


**Figure 1. Flowchart of the study population.** Abbreviations: IPF: Idiopathic pulmonary fibrosis; HS: Healthy subjects; KL-6: Krebs von den Lungen-6; HRCT: High-resolution computed tomography; ROC: Receiver operating characteristic.

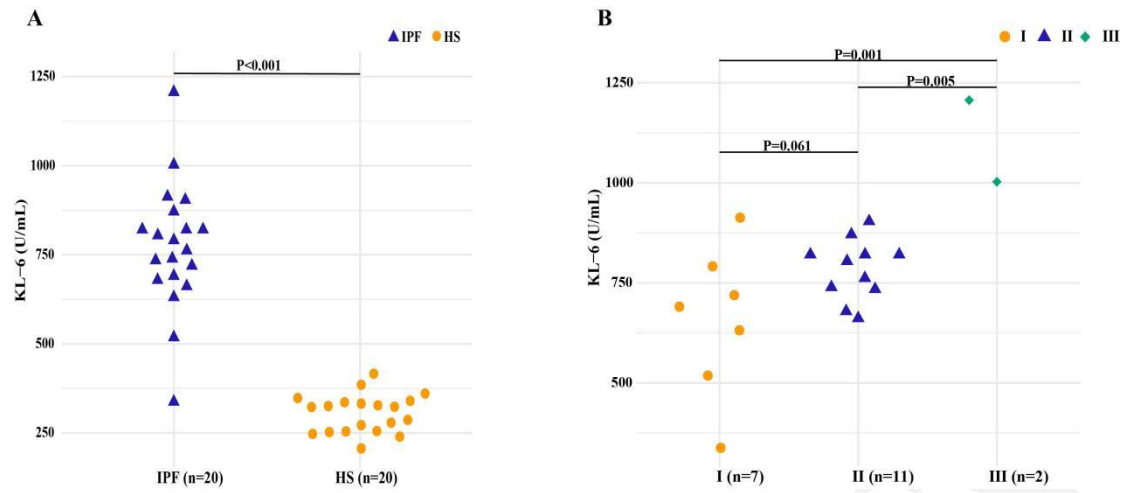


**Figure 2. Induced sputum KL-6 levels in IPF patients and healthy subjects (HS).**

(A) Comparison of induced sputum KL-6 levels between the two groups; (B) Induced sputum KL-6 levels across different GAP stages in the IPF group. Note: Data are presented as scatter plots with individual values. III P75 could not be computed due to small sample size (n=2). Abbreviations: IPF: Idiopathic pulmonary fibrosis; HS: Healthy subjects; KL-6: Krebs von den Lungen-6.

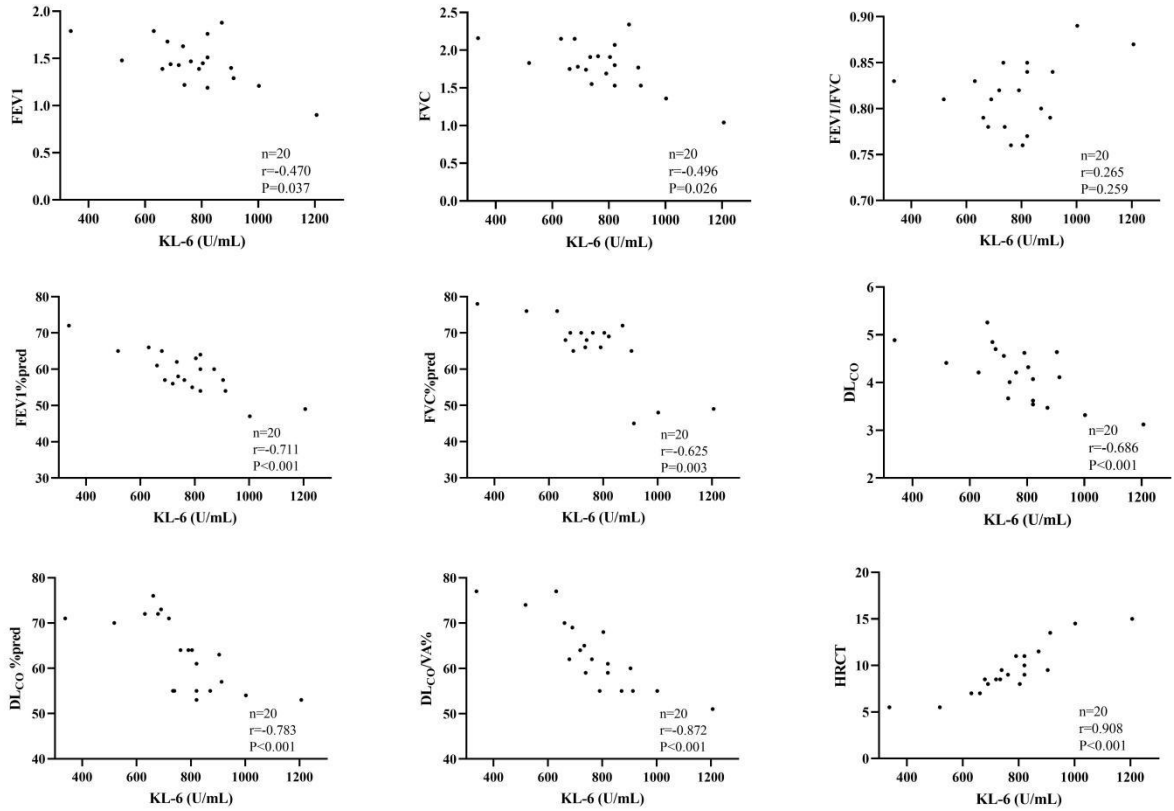


**Figure 3. Correlations between induced sputum KL-6 levels, lung function parameters, and HRCT scores in patients with IPF.** Scatter plots illustrate significant negative correlations between KL-6 and FEV1, FVC, FEV1%pred, FVC%pred, DL<sub>CO</sub>%, DL<sub>CO</sub>%pred, and DL<sub>CO</sub>/VA%, as well as a strong positive correlation with HRCT scores. Corresponding correlation coefficients (r) and *p* values are shown within each panel. Abbreviations: KL-6: Krebs von den Lungen-6; FEV1: Forced expiratory volume in one second; FVC: Forced vital capacity; FEV1/FVC: Ratio of forced expiratory volume in one second to forced vital capacity; DL<sub>CO</sub>: Diffusing capacity of the lung for carbon monoxide; DL<sub>CO</sub>/VA%: Diffusing capacity of the lung for carbon monoxide per unit of alveolar volume; HRCT: High-resolution computed tomography.



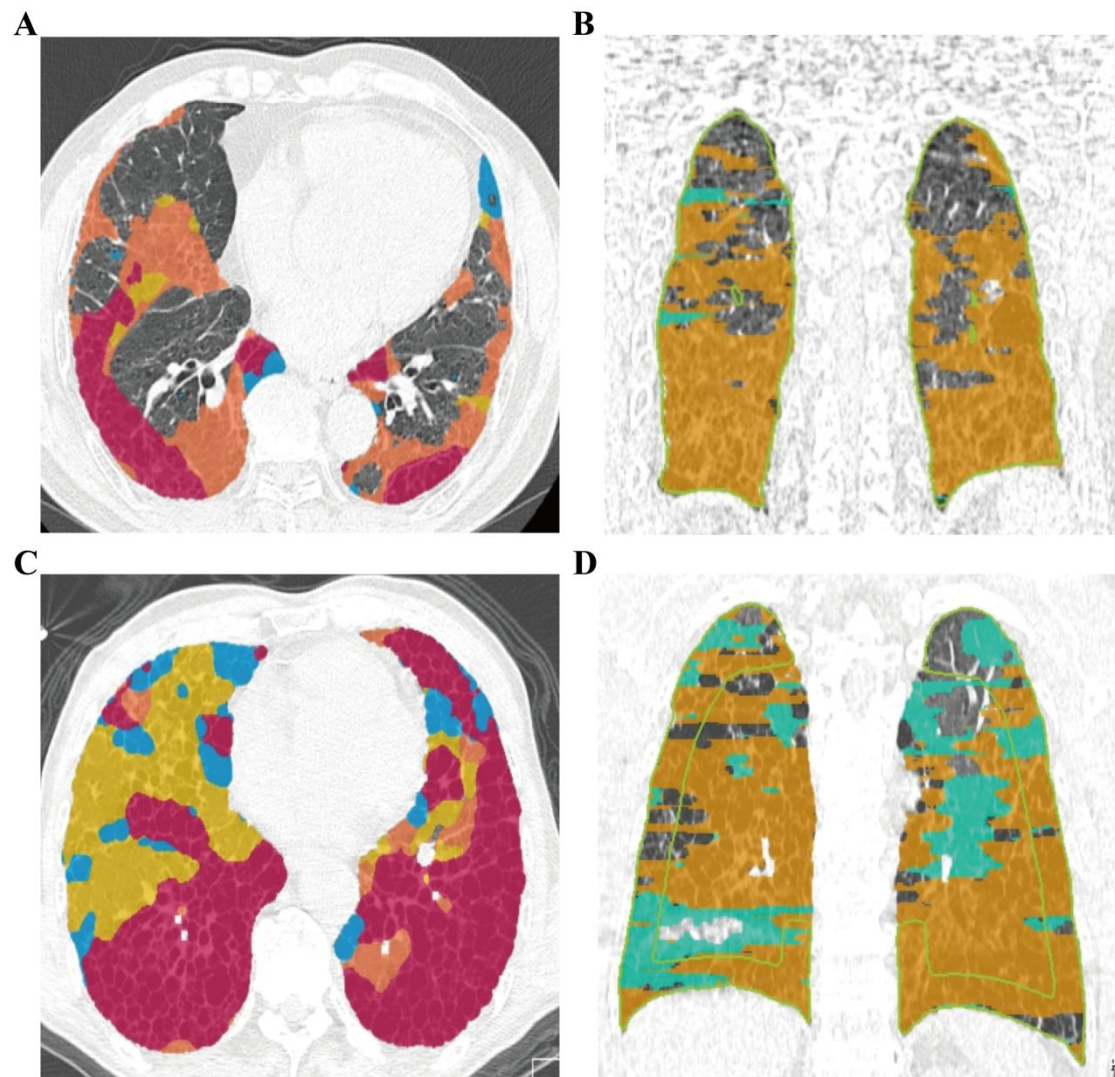


**Figure 4. HRCT assessment of lung fibrosis extent and corresponding induced sputum KL-6 levels in two IPF patients.** (A–B) Patient 1: HRCT revealed a lung fibrosis extent of 15.9%, with an induced sputum KL-6 level of 820.83 U/mL. Fibrotic areas are marked in color. (C–D) Patient 2: HRCT demonstrated a greater fibrosis extent of 31.3%, with a KL-6 level of 1002.63 U/mL, showing a consistent upward trend in KL-6 with increased fibrosis. Abbreviations: HRCT: High-resolution computed tomography; KL-6: Krebs von den Lungen-6; IPF: Idiopathic pulmonary fibrosis.

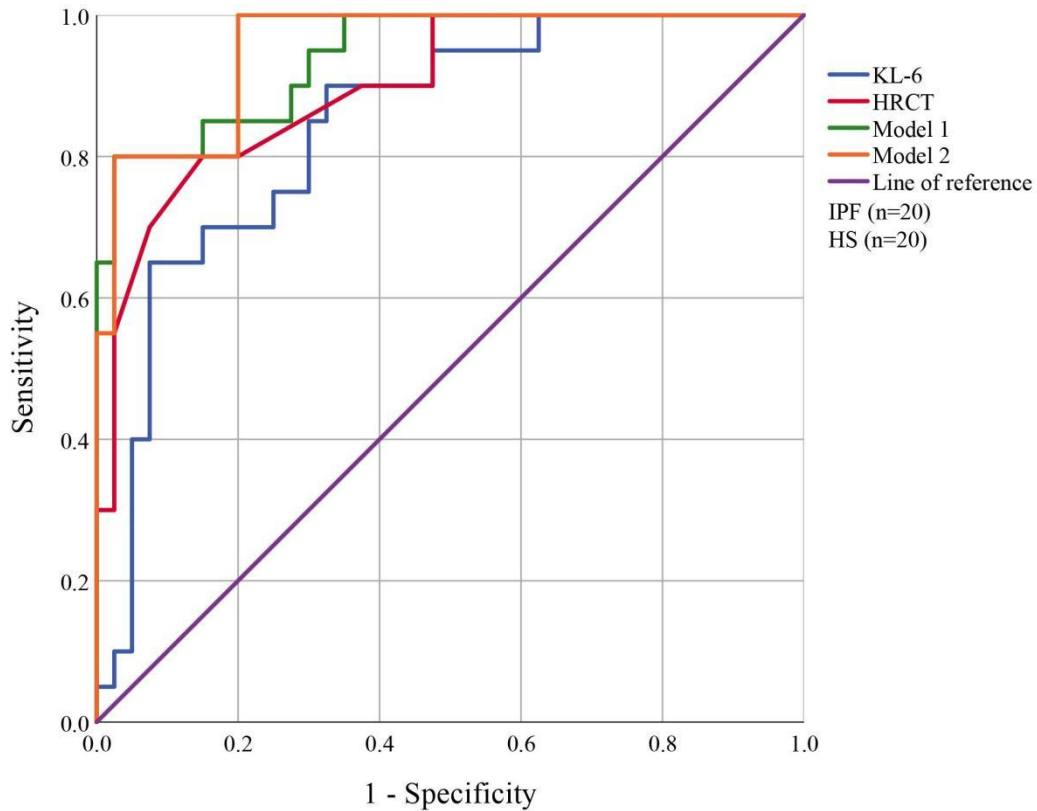


**Figure 5. ROC curves of induced sputum KL-6 and HRCT score in the diagnosis of IPF.** The diagnostic performance of induced sputum KL-6, HRCT score, and their combinations is shown. At a KL-6 threshold of 623.78 U/mL, sensitivity was 90.0%, specificity 67.5%, and AUC 0.844. An HRCT score of 7.75 yielded 80.0% sensitivity, 85.0% specificity, and an AUC of 0.899. Model 1 (KL-6 combined with HRCT) achieved 80.0% sensitivity, 97.5% specificity, and an AUC of 0.936 (95% CI: 0.914–0.944). After adjustment for confounding factors (age and smoking status), Model 2 showed 80.0% sensitivity, 97.5% specificity, and an AUC of 0.940 (95% CI: 0.874–0.956). Abbreviations: ROC: Receiver operating characteristic; IPF: Idiopathic pulmonary fibrosis; HS: Healthy subjects; KL-6: Krebs von den Lungen-6; HRCT: High-resolution computed tomography.

## SUPPLEMENTAL DATA

**Supplementary table 1. Relationship between induced sputum KL-6 and lung function and HRCT score**

	<i>r</i>	<i>p</i> value
FEV1	-0.470	0.037
FVC	-0.496	0.026
FEV1/FVC	0.265	0.259
FEV1 %pred	-0.711	<0.001
FVC %pred	-0.625	0.003
DL <sub>CO</sub>	-0.686	<0.001
DL <sub>CO</sub> %pred	-0.783	<0.001
DL <sub>CO</sub> /VA%	-0.872	<0.001
HRCT	0.908	<0.001

Abbreviations: FEV1: Forced expiratory volume in one second; FVC: Forced vital capacity; FEV1/FVC: Ratio of forced expiratory volume in one second to forced vital capacity; DL<sub>CO</sub>: Diffusing capacity of the lung for carbon monoxide; DL<sub>CO</sub>/VA%: Diffusing capacity of the lung for carbon monoxide per unit of alveolar volume; HRCT: High-resolution computed tomography.